A benchmark study of the vertical electronic spectra of the linear chain radicals C_2H and C_4H

Ryan C. Fortenberry, Rollin A. King, John F. Stanton, and T. Daniel Crawford

View Online

Export Citation

ARTICLES YOU MAY BE INTERESTED IN

A benchmark study of the vertical electronic spectra of the linear chain radicals C_2H and C_4H

Ryan C. Fortenberry,[1] Rollin A. King,[2] John F. Stanton,[3] and T. Daniel Crawford[1,a)]
[1]*Department of Chemistry, Virginia Tech, Blacksburg, Virginia 24061, USA*
[2]*Department of Chemistry, Bethel University, St. Paul, Minnesota 55112, USA*
[3]*Departments of Chemistry and Biochemistry, University of Texas, Austin, Texas 78712, USA*

The ability of coupled-cluster models to predict vertical excitation energies is tested on the electronic states of carbon-chain radicals of particular relevance to interstellar chemistry. Using spin-unrestricted and -restricted reference wave functions, the coupled-cluster singles and doubles (CCSD) model and a triples-including model (CC3) are tested on the σ radicals C_2H and C_4H. Both molecules exhibit low-lying excited states with significant double-excitation character (as well as states of quartet multiplicity) and are thus challenging cases for excited-state approaches. In addition, we employ two diagnostics for the reliability of the CC results: the approximate excitation level (AEL) relative to the ground state and the difference between excitation energies obtained with spin-unrestricted and spin-restricted reference wave functions (the U-R difference). We find that CCSD yields poor excitation energies for states with AEL significantly larger than ca. 1.1 and/or large U-R differences, as well as for certain states exhibiting large spin contamination or other inadequacies in the reference determinant. In such cases, connected triple excitations can be included in the model and generally provide improved results. Furthermore, we find that large discrepancies exist between CC and multireference (MR) results for certain states. These disagreements are not related to basis-set effects, but likely arise from the lack of spin adaptation in conventional spin-orbital CC implementations and active space selection in the MR models. © *2010 American Institute of Physics*. [doi:10.1063/1.3376073]

I. INTRODUCTION

Interstellar chemistry provides a superb example of synergistic interplay between theory and experiment. Almost since its inception, the field of quantum chemistry has played a significant role in the identification of molecules in interstellar and circumstellar media. For many rigid molecules, microwave emissions measured from various sources can be compared to simulated rotational spectra with a high degree of reliability due to the relative ease with which structures and associated rotational constants submit to accurate theoretical prediction.[1] Given that many molecular candidates for identification in interstellar sources are difficult to prepare in laboratories, theoretical methods are even more critical. Early examples of this interplay between measurements [taken from observation in the interstellar medium (ISM) or laboratory experiments] and theoretical computations include the discoveries of N_2H^+ in 1974 (Ref. 2) and C_3N in 1977,[3,4] and such collaborations continue today.[5–7]

For some molecular species in the ISM, particularly those with low abundances, more sensitive methods such as UV/visibility spectroscopy are preferred for identification.[8–10] However, electronic spectra are significantly more difficult than pure rotational spectra to simulate accurately for several reasons.[11] First, both transition frequencies and oscillator strengths exhibit much greater sensitivity to the level of theory employed (especially for open-

shell molecules). Second, vibronic effects are relatively common, but also exceedingly difficult to model,[12–15] and simple comparison of experimental spectra to computed vertical (or even adiabatic) transitions is insufficient for robust assignments. Finally, high levels of electron correlation are often needed to describe excited states that are not comprised primarily of one-electron excitations, even when the ground electronic state is well-described by lower levels of theory. Thus, the obstacles that must be overcome for theory to play a similarly valuable role in the identification of interstellar compounds via electronic spectroscopy as it does for microwave spectroscopy are daunting. Nevertheless, ongoing efforts to identify, for example, the carriers of the diffuse interstellar bands (DIBs),[16–20] the mysterious series of visible and near-infrared lines whose provenance still remains unknown, may very well hinge on advances in the reliability of quantum chemical models.

This work focuses on the last of the three factors described above, viz. the level of electron correlation required to provide an accurate description of the ground and excited electronic wave functions involved in a given transition. In particular, we consider the application of coupled-cluster theory[21,22]—widely regarded as one of the most reliable quantum chemical models[23,24]—to electronic excitations in radicals, where correlation effects are often paramount. The highest level of theory employed in this work is CC3, which was developed in the 1990s for the description of response properties[25–27] and was extended to open-shell species in

a)Electronic mail: crawdad@vt.edu.

2005.[28] For a test set, we have chosen two linear molecules of importance to interstellar chemistry: C_2H and C_4H. These radicals were discovered in the ISM in 1974 (Ref. [29]) and 1978,[30] respectively, the latter study aided by comparison to theoretically computed rotational constants. Related $C_{2n}H$ $(n=1,2,\ldots)$ carbon-chain molecules have been proposed as one of several possible carriers of the DIBs.[31–36] C_2H is also reported to be potentially among the most abundant molecules in the universe after the much more common carbon monoxide and the ubiquitous hydrogen molecule.[37] Additionally, both C_2H and C_4H are believed to play a role in the chemistry of extraterrestrial planetary atmospheres, especially that of Saturn's moon Titan.[38] For our purposes, however, these two molecules exhibit both valence and Rydberg excitations, including states with strong double-excitation character and higher spin multiplicities,[39] and therefore provide a significant challenge to *ab initio* methods.[40–45]

II. COMPUTATIONAL DETAILS

Structural optimizations of each radical were carried out at the coupled-cluster singles, doubles, and perturbative triples [CCSD(T)] level of theory,[46] in conjunction with a variety of open-shell reference wave functions based on Hartree–Fock determinants, including spin-unrestricted (UHF),[47,48] spin-restricted open-shell (ROHF),[49–52] and quasirestricted (QRHF) (Ref. [53]) formulations. In addition, the optimized structures were computed using the equation-of-motion coupled-cluster method for ionized states (EOMIP-CCSD),[54] in which the anions C_2H^- and C_4H^- provide the starting coupled-cluster wave functions. All computations were carried out in the C_{2v} subgroup of $C_{\infty v}$. Dunning's triple-zeta correlation-consistent basis set, cc-pVTZ,[55] was used to obtain the optimized geometries.

Vertical excitation energies were computed at the UHF-CCSD(T)/cc-pVTZ optimized structures using the equation-of-motion CCSD (EOM-CCSD) approach[56–59] as well as an open-shell extension[28] of the approximate triples method, CC3 of Koch, Christiansen, Jørgensen, and co-workers.[25] Both levels of theory used UHF and ROHF reference determinants with the carbon $1s$ electrons frozen for each radical. The lowest several $\Sigma^+(A_1)$, $\Sigma^-(A_2)$, $\Delta(A_1/A_2)$, and $\Pi(B_1/B_2)$ states were computed using a multiroot method at the CCSD level and a root-following approach with CC3 (whose quasieigenvalue implementation precludes computation of more than one root at a time but avoids the storage of triples wave function amplitudes).[28] For comparison to the results from high-level coupled-cluster models, vertical excitation energies were also computed with configuration interaction singles (CIS) (Ref. [60]) and time-dependent density functional theory (TD-DFT)[61] using the Becke three-parameter exchange functional[62] with the Lee–Yang–Parr correlation functional[63] (B3LYP).[64] All coupled-cluster computations were carried out with the PSI3 (Ref. [65]) and CFOUR (Ref. [66]) quantum chemical program packages. CIS and B3LYP computations were carried out with the GAUSSIAN03 package.[67]

For the excited-state computations at the various levels of theory, correlation-consistent basis sets including diffuse functions were employed, including the aug-cc-pVDZ, aug-
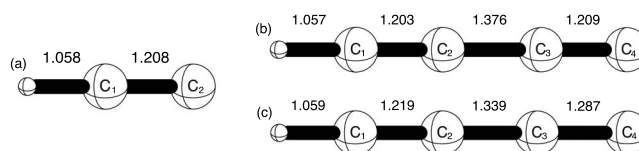

FIG. 1. UHF-CCSD(T)/cc-pVTZ optimized linear structures (bond distances in angstroms) of (a) C_2H ($^2\Sigma^+$); (b) C_4H ($^2\Sigma^+$); and (c) C_4H ($^2\Pi$) radicals.

cc-pVTZ, and d-aug-cc-pVDZ basis sets.[55,68] The impact of further augmentation of the basis set was analyzed by adding new diffuse functions (s, p, and d sets for carbon, and s and p for hydrogen) obtained by even-tempered extrapolation of the most diffuse exponents in each angular momentum of the d-aug-cc-pVDZ basis sets for C and H to yield what will be referred to in this paper as the t-aug-cc-pVDZ basis. For carbon, the diffuse functions added to the d-aug-cc-pVDZ basis to produce the t-aug-cc-pVDZ basis were $\alpha_s=0.004\,060\,6$, $\alpha_p=0.002\,886\,4$, and $\alpha_d=0.011\,406$; for hydrogen, $\alpha_s=0.001\,767\,4$ and $\alpha_p=0.005\,285\,7$.

III. RESULTS AND DISCUSSION

A. Optimized geometries

The UHF-CCSD(T)/cc-pVTZ optimized structure of the ground state of the ethynyl radical (C_2H) is given in Fig. 1. C_2H has a ground-state $^2\Sigma^+$ term,[40–44,69–74] which suggests that its structure should be comparable to acetylene. Indeed, the UHF-CCSD(T)/cc-pVTZ C–C triple bond of 1.208 Å resembles that of acetylene, whose RHF-CCSD(T)/cc-pVTZ C–C bond is somewhat shorter at 1.206 Å. We note that the ROHF-CCSD(T), EOMIP-CCSD, and QRHF-CCSD(T) methods, as well as earlier RCCSD(T)/cc-pVTZ computations by Woon[43] all agree with this result. We also note that the UHF reference function for this state exhibits substantial spin contamination, as evidenced by its large expectation value of $\hat{S}^2$ of 1.13, though the CCSD wave function for the $^2\Sigma^+$ state constructed from either the UHF or ROHF determinant yields very little contamination, with corresponding expectation values of 0.758 and 0.752, respectively.[75,76]

For the longer C_4H chain, nearly all of the theoretical methods employed here [with the notable exception of ROHF-CCSD(T)] predict a $^2\Pi$ ground state. In spite of this, we elected to use the UHF-CCSD(T)/cc-pVTZ optimized structure of the lowest energy $^2\Sigma^+$ state as the starting point of our study for three reasons: (1) the lowest $^2\Sigma^+$ and $^2\Pi$ states have been shown by both theory[43–45,71,72,77,78] and experiment[79–84] to be nearly degenerate with experiment favoring the former; (2) this choice gives greater ease of comparison of the vertical transitions between C_2H and C_4H; and (3) the purpose of this work is to benchmark high-level coupled-cluster vertical excitation energies rather than to reproduce the experimental spectra.

As shown in Fig. 1, UHF-CCSD(T)/cc-pVTZ predicts an optimized structure of the $^2\Sigma^+$ state to be similar to the shorter C_2H chain. The H–C_1 bond and the C_3–C_4 bond in C_4H (1.057 and 1.209 Å, respectively) vary from their C_2H counterparts by less than 0.002 Å each. The C_1–C_2 bond of C_4H is predicted to be 1.203 Å, varying by 0.006 Å from the

C–C bond of C_2H. In addition, this lowest energy $^2\Sigma^+$ state of C_4H is clearly seen to resemble the structure of diacetylene. The C_2-C_3 bond of C_4H is 1.376 Å, a slight deviation from RHF-CCSD(T)/cc-pVTZ diacetylene at 1.370 Å. The C_1-C_2 bond in diacetylene measures a length of 1.212 Å, just 0.009 Å longer than the same bond in C_4H. The spin contamination of the UHF reference function is even larger in the $^2\Sigma^+$ state of C_4H than in C_2H, with a poor $\langle \hat{S}^2 \rangle$ value of 1.59, though, again, the UHF- and ROHF-CCSD wave functions produce much more reasonable values of 0.782 and 0.755, respectively.

In comparison, the structures of the lowest $^2\Sigma^+$ and $^2\Pi$ states of C_4H most closely resemble those of diacetylene and the corresponding cumulene, respectively. The C_1-C_2 bond of the $^2\Sigma^+$ state is 0.017 Å shorter than that of the $^2\Pi$ state while the C_2-C_3 bond is longer for the $^2\Sigma^+$ state by 0.037 Å, as illustrated in Fig. 1. The C_3-C_4 bond length shows the most variation between the states and is 0.077 Å longer for the $^2\Pi$ state.

B. Vertical excitation energies

In this section, we analyze vertical excitation energies for the C_2H and C_4H radicals using the methods described earlier. Spin remains one of the central obstacles in the application of conventional CC methods to excited states of open-shell species. In the following sections, the spin-symmetry assignments of the individual states are approximate in that the formulation of open-shell coupled-cluster theory employed in this work does not yield eigenfunctions of the $\hat{S}^2$ operator, though, in some cases, the dominant doublet versus quartet character of many states can be estimated by examination of the expectation value of $\hat{S}^2$ and of the relevant determinantal contributions. Nevertheless, as discussed previously by Szalay and Gauss,[85] the lack of spin adaptation in standard formulations of excited-state coupled-cluster theory can result in the exaggerated importance of so-called "pseudotriple" (and possibly higher) excitations, in which a double excitation is accompanied by a spin-flip within the open-shell orbital(s). While such terms would appear naturally as doubles in a fully spin-adapted formulation, spin-orbital approaches, such as that applied in this work, require at least triple excitations to describe them in even a qualitatively correct manner.

In an effort to develop an understanding of the accuracy to be expected from the CCSD and CC3 methods for open-shell species, we will consider two diagnostics for the reliability of the EOM-CCSD data. The first is the difference between UHF- and ROHF-based results (which we will refer to here as the "U-R" difference). As the level of electron correlation is increased, the U-R difference typically decreases (and is zero at the full-CI limit); hence large differences warrant skepticism in the given results. Second, we compute an "approximate excitation level" (AEL) based on the projection of the excited-state wave function onto the singles and doubles space. For CCSD, the AEL we employ is defined as

$$
\begin{aligned}
\text{AEL} &\equiv \langle \tilde{\Psi}_{\text{CCSD}} | S \rangle \langle S | \Psi_{\text{CCSD}} \rangle + 2 \langle \tilde{\Psi}_{\text{CCSD}} | D \rangle \langle D | \Psi_{\text{CCSD}} \rangle \\
&= \sum_{ia} \langle \Phi_0 | \mathcal{L} e^{-T} | \Phi_i^a \rangle \langle \Phi_i^a | \mathcal{R} e^T | \Phi_0 \rangle + 2 \\
&\quad \times \sum_{i>j,a>b} \langle \Phi_0 | \mathcal{L} e^{-T} | \Phi_{ij}^{ab} \rangle \langle \Phi_{ij}^{ab} | \mathcal{R} e^T | \Phi_0 \rangle,
\end{aligned} \tag{1}
$$

where Φ_0, Φ_i^a, and Φ_{ij}^{ab} denote the reference and excited determinants, and the tilde differentiates left- and right-hand EOM-CCSD excited states, which are parametrized in terms of the $\mathcal{L}$ and $\mathcal{R}$ cluster operators, respectively. EOM-CCSD AEL values significantly larger than 1.0 suggest appreciable double-excitation character in the excited-state wave function. In such cases, EOM-CCSD is generally expected to yield poor results, and higher-level correlation treatments are necessary. Furthermore, as noted by Szalay and Gauss,[85] for cases exhibiting significant contributions from pseudotriple excitations, even states dominated by single excitations can have significant errors, and thus the question of the usefulness of methods that include the effects of connected triple excitations, such as CC3, remains open.

We also note that the AEL of Eq. (1) differs from the form given by Stanton and Bartlett,[56] who defined the diagnostic in terms of differences between approximate natural-orbital occupation numbers of the ground and excited states. However, we have found that this definition can yield AELs less than 1.0 in many cases. The above definition, however, may be viewed as measuring the overall excitation level relative to the reference determinant rather than the CCSD wave function, and is less likely (though still not guaranteed, at least for totally symmetric excitations) to produce values under unity. In addition, the above AEL definition avoids any ambiguity as to the use of relaxed or unrelaxed densities. In passing, we note that the singles and doubles projections that comprise this diagnostic have been computed by the ACESII/CFOUR program package for more than a decade without being published in the literature.

1. C_2H

Table I reports vertical excitation energies, excited-state characters, and AELs (*vide infra*) for 16 states of C_2H at the CCSD and CC3 levels of theory with the aug-cc-pVDZ basis set. The term assignments in the table are based on examination of the determinantal components of the excited-state wave function (the specific coefficients given in the table are taken from the ROHF-CC3 level) as well as the $\hat{S}^2$ expectation reported in Table II. The canonical molecular orbital (MO) transitions given for each excitation are relative to the ground $^2\Sigma^+$ state, which has the Hartree–Fock configuration of (core) $3\sigma^2 4\sigma^2 1\pi^4 5\sigma$. The key virtual MOs for the states given in the table are the singly occupied 5σ, the valence $2\pi^*$, and four low-lying Rydberg orbitals: $3s$, $3p\sigma$, and a pair of nearly degenerate $3p\pi$ orbitals (each centered on a different carbon atom). Some higher-lying states given in the tables include minor contributions into Rydberg $4s$, $4p\sigma$, and even $5p\sigma$ orbitals. Transitions of significance are considered to be those with coefficients whose absolute magnitudes exceed 0.20 for single excitations (labeled as either α or β) and 0.10 for double excitations (labeled as $\alpha\beta$, $\alpha\alpha$, or $\beta\beta$).

TABLE I. Vertical excitation energies (eV), state assignments, characters, and AELs (from the ROHF-CCSD level) of C_2H relative to the ground $^2\Sigma^+$ state at various levels of theory with the aug-cc-pVDZ basis set.

State assignment	Excitation character		Vertical excitation energy				AEL
			UHF-CCSD	UHF-CC3	ROHF-CCSD	ROHF-CC3	
$1\ ^2\Pi$	$1\pi\rightarrow5\sigma$	$(0.85\ \beta)$	0.997	0.826	0.798	0.768	1.08
	$1\pi\rightarrow3p\sigma$	$(0.29\ \beta)$					
	$1\pi\rightarrow3s$	$(0.20\ \beta)$					
	$1\pi\rightarrow2\pi^*\ 1\pi\rightarrow5\sigma$	$(0.11\ \alpha\beta)$					
$1\ ^4\Sigma^+$	$1\pi\rightarrow2\pi^*$	$(0.31\ \alpha;\ 0.33\ \beta;\ 0.20\ \alpha\beta)$	5.476	5.306	5.381	5.235	1.14
	$1\pi\rightarrow3p\pi$	$(0.29\ \alpha;\ 0.23\ \beta;\ 0.18\ \alpha\beta)$					
$1\ ^4\Delta$	$1\pi\rightarrow2\pi^*$	$(0.32\ \alpha;\ 0.32\ \beta;\ 0.17\ \alpha\beta)$	6.570	6.382	6.498	6.318	1.13
	$1\pi\rightarrow3p\pi$	$(0.31\ \alpha;\ 0.25\ \beta;\ 0.17\ \alpha\beta)$					
$1\ ^4\Sigma^-$	$1\pi\rightarrow3p\pi$	$(0.35\ \alpha;\ 0.26\ \beta;\ 0.18\ \alpha\beta)$	7.353	7.139	7.272	7.067	1.13
	$1\pi\rightarrow2\pi^*$	$(0.31\ \alpha;\ 0.30\ \beta;\ 0.16\ \alpha\beta)$					
$2\ ^2\Sigma^+$	$4\sigma\rightarrow5\sigma$	$(0.36\ \beta)$	8.354	7.555	8.067	7.334	1.54
	$1\pi\rightarrow2\pi^*$	$(0.31\ \alpha\beta)$					
	$1\pi\rightarrow3p\pi$	$(0.30\ \alpha\beta)$					
$1\ ^2\Sigma^-$	$1\pi\rightarrow3p\pi$	$(0.36\ \alpha;\ 0.32\ \beta)$	7.664	7.575	7.652	7.578	1.05
	$1\pi\rightarrow2\pi^*$	$(0.32\ \alpha;\ 0.34\ \beta)$					
$1\ ^2\Delta$	$1\pi\rightarrow3p\pi$	$(0.40\ \alpha;\ 0.31\ \beta)$	7.990	7.903	7.976	7.898	1.06
	$1\pi\rightarrow2\pi^*$	$(0.32\ \alpha;\ 0.29\ \beta)$					
$2\ ^2\Pi$ [a]	$1\pi\rightarrow3s$	$(0.39\ \beta)$	8.410	8.258/8.299[a]	8.444	8.195/8.315[a]	1.07
	$1\pi\rightarrow2\pi^*\ 1\pi\rightarrow5\sigma$	$(0.33\ \alpha\beta;\ 0.30\ \alpha\beta;\ 0.28\ \beta\beta)$					
	$1\pi\rightarrow3p\pi\ 1\pi\rightarrow5\sigma$	$(0.31\ \alpha\beta;\ 0.29\ \alpha\beta;\ 0.19\ \beta\beta)$					
	$1\pi\rightarrow4s$	$(0.20\ \beta)$					
$3\ ^2\Pi$	$1\pi\rightarrow3s$	$(0.72\ \alpha;\ 0.09\ \beta;\ 0.29\ \alpha\beta)$	8.852	8.625	8.810	8.519	1.12
	$1\pi\rightarrow4s$	$(0.31\ \alpha;\ 0.12\ \alpha\beta)$					
	$1\pi\rightarrow2\pi^*\ 1\pi\rightarrow5\sigma$	$(0.13\ \alpha\beta;\ 0.19\ \beta\beta)$					
	$1\pi\rightarrow3p\pi\ 1\pi\rightarrow5\sigma$	$(0.12\ \alpha\beta;\ 0.13\ \beta\beta)$					
	$5\sigma\rightarrow3s\ 1\pi\rightarrow3p\sigma$	$(0.12\ \alpha\beta)$					
$3\ ^2\Sigma^+$	$4\sigma\rightarrow5\sigma$	$(0.67\ \beta)$	9.334	8.660	9.137	8.525	1.45
	$1\pi\rightarrow2\pi^*$	$(0.23\ \beta)$					
	$1\pi\rightarrow3p\pi\ 1\pi\rightarrow5\sigma$	$(0.16\ \alpha\beta)$					
	$1\pi\rightarrow2\pi^*\ 1\pi\rightarrow5\sigma$	$(0.15\ \alpha\beta)$					
$1\ ^4\Pi$	$1\pi\rightarrow3p\sigma$	$(0.49\ \beta)$	9.016	8.881	9.027	8.805	1.08
	$1\pi\rightarrow3s$	$(0.32\ \beta)$					
	$1\pi\rightarrow2\pi^*\ 1\pi\rightarrow5\sigma$	$(0.23\ \alpha\beta;\ 0.18\ \alpha\beta;\ 0.25\ \beta\beta)$					
	$1\pi\rightarrow4p\sigma$	$(0.24\ \beta)$					
	$1\pi\rightarrow3p\pi\ 1\pi\rightarrow5\sigma$	$(0.23\ \alpha\beta;\ 0.18\ \alpha\beta;\ 0.17\ \beta\beta)$					
	$1\pi\rightarrow5p\sigma$	$(0.22\ \beta)$					
$4\ ^2\Pi$	$1\pi\rightarrow3p\sigma$	$(0.62\ \alpha;\ 0.38\ \beta;\ 0.22\ \alpha\beta)$	9.455	9.204	9.403	9.189	1.13
	$1\pi\rightarrow4p\sigma$	$(0.29\ \alpha;\ 0.19\ \beta;\ 0.13\ \alpha\beta)$					
	$1\pi\rightarrow2\pi^*\ 1\pi\rightarrow5\sigma$	$(0.11\ \beta\beta)$					
	$1\pi\rightarrow3p\pi\ 1\pi\rightarrow5\sigma$	$(0.10\ \alpha\beta)$					
	$5\sigma\rightarrow3p\sigma\ 1\pi\rightarrow3p\sigma$	$(0.10\ \alpha\beta)$					
$2\ ^4\Sigma^+$	$1\pi\rightarrow3p\pi$	$(0.36\ \alpha;\ 0.48\ \beta;\ 0.26\ \beta;\ 0.14\ \alpha\beta)$	9.568	9.457	9.579	9.429	1.07
$5\ ^2\Pi$	$5\sigma\rightarrow3p\pi$	$(0.56\ \alpha)$	9.712	9.405	9.644	9.516	1.18
	$5\sigma\rightarrow2\pi^*$	$(0.48\ \alpha)$					
	$1\pi\rightarrow3p\pi\ 1\pi\rightarrow5\sigma$	$(0.28\ \alpha\beta;\ 0.17\ \alpha\beta;\ 0.10\ \beta\beta)$					
	$1\pi\rightarrow2\pi^*\ 1\pi\rightarrow5\sigma$	$(0.25\ \alpha\beta;\ 0.17\ \alpha\beta;\ 0.13\ \beta\beta)$					
$2\ ^2\Delta$	$1\pi\rightarrow3p\pi$	$(0.61\ \beta;\ 0.29\ \beta)$	9.634	9.550	9.660	9.541	1.09
$2\ ^2\Sigma^-$	$1\pi\rightarrow3p\pi$	$(0.58\ \beta;\ 0.32\ \beta)$	9.765	9.663	9.796	9.665	1.06

[a]Two possible $^2\Pi$ states in this energy range were identified at the CC3 level. See text for discussion.

In the Hartree–Fock MO basis, nearly all of the states reported in Table I involve more than one significant transition, and all exhibit at least some Rydberg character. The lowest excited state corresponds to the $A\ ^2\Pi\leftarrow X\ ^2\Sigma^+$ transition, whose largest contribution arises from β-spin excitation from the 1π orbital into the singly occupied 5σ, though single excitations into the $3p\sigma$ and $3s$ Rydberg orbitals (as

well a valence-MO double excitation) all make nonnegligible contributions. The computed excitation energy for this state depends significantly on the choice of reference determinant, as indicated by the U-R difference of 0.2 eV. At the CC3 level of theory, the U-R difference is reduced, as expected (to 0.06 eV), and the larger CCSD to CC3 shift is observed for the UHF reference function. The AEL for this

TABLE II. $\langle \hat{S}^2 \rangle$ values of excited states of C_2H at the EOM-CCSD/aug-cc-pVDZ level of theory. States marked in italics involve unbalanced contributions from low-spin determinants depicted schematically in Fig. 2.

State	UHF-EOM-CCSD	ROHF-EOM-CCSD
1 $^2\Pi$	0.786	0.754
1 $^4\Sigma^+$	3.478	3.509
1 $^4\Delta$	3.403	3.484
1 $^4\Sigma^-$	3.241	3.393
2 $^2\Sigma^+$	1.064	0.936
1 $^2\Sigma^-$	0.893	0.817
1 $^2\Delta$	0.781	0.761
2 $^2\Pi$	*2.095*	*2.213*
3 $^2\Pi$	*2.032*	*1.900*
3 $^2\Sigma^+$	1.028	0.844
1 $^4\Pi$	*2.214*	*2.434*
4 $^2\Pi$	*1.553*	*1.439*
2 $^4\Sigma^+$	*2.783*	*2.937*
5 $^2\Pi$	0.989	0.824
2 $^2\Delta$	*1.941*	*1.920*
2 $^2\Sigma^-$	*1.813*	*1.807*

state (reported in the table for the ROHF-CCSD level) is only 1.08. Koures and Harding[42] reported vertical excitation energies for C_2H at the MRCISD(+Q)/DZP level of theory, and identified the 1 $^2\Pi$ state at 0.60 eV above the ground $^2\Sigma^+$ state, approximately 0.2 eV lower than the CC3 results given in Table I. While Koures and Harding adopted procedures by which they carried out separate computations of the valence and Rydberg states (the latter using MCSCF orbitals adopted from the corresponding anion), all of the states were obtained in the current work using a single basis set and method. This results in mixed valence/Rydberg character for nearly every state. We note further that the B3LYP/aug-cc-pVDZ level of theory, which is normally expected to underestimate excitation energies, yields a corresponding excitation energy of 0.6 eV, in very close agreement with Koures and Harding, while the CIS/aug-cc-pVDZ method gives the same transition significantly in error at 3.4 eV.

The next transition is to a $^4\Sigma^+$ state, for which our assignment of the spin multiplicity arises because of the presence of the significant "spin-flip" $\alpha\beta$ double excitations noted in Table I and its high $\hat{S}^2$ expectation value of ca. 3.5 (just below the pure quartet value of 3.75) reported in Table II.[85] Again, this state exhibits significant Rydberg character in the Hartree–Fock MO basis, with dominant contributions from the valence $2\pi^*$ and Rydberg $3p\pi$ MOs. The EOM-CCSD U-R difference is less than 0.1 eV (a value that is further reduced at the CC3 level) and the AEL is relatively small at 1.14. Again, the ROHF-CC3 method yields the lowest excitation energy at 5.24 eV, but still 0.4 eV higher than that reported by Koures and Harding[42] at the MRCISD(+Q)/DZP level. The next transition is to a $^4\Delta$ state, which also exhibits a small U-R difference and a small AEL, but the ROHF-CC3 excitation energy (6.32 eV) is more than 0.3 eV higher than that reported by Koures and Harding.

Beyond the lowest few states, the agreement between our results and those reported by Koures and Harding[42] de-

teriorates rapidly, both in the ordering of the states and the excitation energies. The next six states according to ROHF-CC3 theory are $^4\Sigma^-$, $^2\Sigma^+$, $^2\Sigma^-$, $^2\Delta$, $^2\Pi$, and $^2\Pi$, while Koures and Harding report $^4\Pi$, $^4\Sigma^-$, $^2\Sigma^+$, $^2\Pi$, $^2\Sigma^-$, and $^2\Delta$. Most significantly, Koures and Harding find the $^4\Pi$ state at 6.59 eV, while CC theory places a state with the same assignment more than 2 eV higher at 8.81 eV (at the ROHF-CC3 level). Our assignment of a quartet to this Π state is tentative and based primarily on the $\hat{S}^2$ expectation values reported in Table II of 2.21 and 2.43 for UHF- and ROHF-EOM-CCSD, respectively, which lie midway between pure doublet (0.75) and pure quartet (3.75) values. This state exhibits a U-R difference at the EOM-CCSD level of 0.01 eV (which, notably, increases slightly at the CC3 level to 0.08 eV) and a relatively small AEL of 1.08, and the shift from ROHF-CCSD to ROHF-CC3 is 0.22 eV. Clearly spin contamination is the major source of the discrepancy between the CC and MRCI results for this case.

The lowest two $^2\Sigma^+$ excited states have the largest AELs (1.54 and 1.45, respectively) of all the states identified in Table I. The lower state at 7.33 eV (ROHF-CC3) exhibits nearly equal contributions from the $4\sigma \rightarrow 5\sigma$ (α-spin single excitation), $1\pi \rightarrow 2\pi^*$ ($\alpha\beta$ double excitation), and $1\pi \rightarrow 3p\pi$ ($\alpha\beta$ double excitation) transitions, while the higher state at 8.53 eV (ROHF-CC3) is more strongly dominated by the $4\sigma \rightarrow 5\sigma$ contribution (with smaller double-excitation contributions involving the $3p\pi$ and $2\pi^*$ orbitals). The U-R difference in both cases is 0.2–0.3 eV at the CCSD level, and the difference between the MRCISD(+Q)/DZP and ROHF-CC3 excitation energies for these states is slightly larger: 0.6 eV for the lower and 0.4 for the upper.[42]

We also take special note of the second $^2\Pi$ state, which Koures and Harding identify at 7.29 eV. CC methods place this state much higher in energy (at least 8.195 eV with the aug-cc-pVDZ basis set). However, the CC3 computations identified two distinct $^2\Pi$ states in this energy regime. Specifically, the root-following method used in the CC3 approach employed in PSI3 uses a set of EOM-CCSD excited states as initial guesses and follows the root chosen by the user for the CC3 procedure. To avoid root-flipping problems, the program identifies the desired root in each iteration based on the overlap between its singles and doubles components with the selected EOM-CCSD wave function. This procedure typically yields CC3 excited states that compare well with their EOM-CCSD counterparts. However, in the search for $^2\Pi$ states, a computation requesting a higher-lying root (the eighth excited state in the b_1 irrep of C_{2v}) exhibited collapse to a lower root that did not compare well to the original EOM-CCSD guess upon convergence. Thus, we have reported both excitation energies—one from the initial pass and one from the higher-root search—in the CC3 columns of Table I, though it should be emphasized that the ROHF-CC3 excitation character given in the table for this state does not match well with the corresponding EOM-CCSD states. (More specifically, the CC3 states exhibit much larger double-excitation character than those from EOM-CCSD.) Regardless, the comparison between the ROHF-CC3 (8.20 eV) and MRCISD(+Q)/DZP (8.17 eV) excitation en-

TABLE III. Vertical excitation energies (eV), state assignments, and AELs of C_2H relative to the ground $^2\Sigma^+$ state at the EOM-CCSD level of theory with the aug-cc-pVTZ, d-aug-cc-pVDZ, and t-aug-cc-pVDZ basis sets.

State assignment	aug-cc-pVTZ			d-aug-cc-pVDZ		t-aug-cc-pVDZ	
	UHF	ROHF	AEL	UHF	ROHF	UHF	ROHF
$1\ ^2\Pi$	0.989	0.766	1.08	0.982	0.781	0.997	0.797
$1\ ^4\Sigma^+$	5.531	5.437	1.12	5.478	5.383	5.474	5.380
$1\ ^4\Delta$	6.541	6.467	1.12	6.570	6.498	6.568	6.496
$1\ ^4\Sigma^-$	7.320	7.241	1.11	7.349	7.268	7.350	7.269
$2\ ^2\Sigma^+$	8.465	8.186	1.47	8.360	8.073	8.354	8.067
$1\ ^2\Sigma^-$	7.564	7.537	1.06	7.659	7.646	7.660	7.648
$1\ ^2\Delta$	7.912	7.889	1.06	7.981	7.967	7.985	7.971
$2\ ^2\Pi$	8.511	8.545	1.07	8.364	8.396	8.367	8.398
$3\ ^2\Pi$	8.938	8.904	1.11	8.787	8.753	8.791	8.756
$3\ ^2\Sigma^+$	9.485	9.244	1.54	9.335	9.132	9.176	9.130
$1\ ^4\Pi$	9.068	9.081	1.08	8.892	8.905	8.896	8.910
$4\ ^2\Pi$	9.500	9.441	1.13	9.336	9.284	9.341	9.289
$2\ ^4\Sigma^+$	9.547	9.561	1.07	9.181	9.209	9.329	9.205
$5\ ^2\Pi$	9.709	9.608	1.15	9.685	9.615	9.676	9.607
$2\ ^2\Delta$	9.580	9.612	1.06	9.197	9.231	9.192	9.226
$2\ ^2\Sigma^-$	9.690	9.722	1.06	9.273	9.306	9.268	9.302

ergies for this state are significantly better, assuming, of course, that this state corresponds to the lowest $^2\Pi$ Rydberg state reported by Koures and Harding.[42]

The discrepancies between CC and MRCISD most likely arise from two points. First, as noted earlier, the open-shell CC approach employed in this work lacks spin-adaptation of the excited-state wave functions. In particular, at the EOM-CCSD level of theory, spin-orbital implementations fail to include pseudotriple excitations,[85] which are essential for a balanced treatment of electron-correlation effects between the ground and excited state. Large shifts between CCSD and CC3, such as that observed for the $2\ ^2\Sigma^+$ state (0.8 eV for the UHF reference) are partly due to such contributions, though the perturbative CC3 method cannot be expected to account for them completely (and improved electron-correlation balance may require even higher excitations). Second, the discrepancies may also be related to the choice of active space in the MRCISD computations, which included five electrons in five orbitals for the valence states and five electrons in seven orbitals for the Rydberg states.[42]

In order to examine basis-set dependence on the excited states, additional ROHF- and UHF-EOM-CCSD computations were carried out. Table III summarizes EOM-CCSD/ aug-cc-pVTZ, /d-aug-cc-pVDZ, and /t-aug-cc-pVDZ vertical excitation energies for the same 16 excited states (given in the same order as in Table I). The basis-set dependence of states dominated by valence-orbital transitions is small, e.g., the largest shift between aug-cc-pVDZ and aug-cc-pVTZ is 0.151 eV occurring for the $3\ ^2\Sigma^+$ state. For states exhibiting substantial Rydberg character, additional diffuse functions yield significant lowering of the excitation energies, particularly for the high-lying $2\ ^4\Sigma^+$, $2\ ^2\Delta$, and $2\ ^2\Sigma^-$ states. However, the extension of the diffuse space beyond d-aug-cc-pVDZ has essentially no impact, even for these states. Furthermore, while the MRCISD(+Q)/DZP excitation energies of Koures and Harding are invariably lower than their CC counterparts reported here, the improvement in the basis

set actually increases the excitation energy in several of the states in Table III, indicating that basis-set effects are not the source of the discrepancies between CC and MRCI.

2. C_4H

Table IV reports vertical excitation energies, excited-state characters, and AELs for 13 states of C_4H below 8 eV at the CCSD and CC3 levels of theory, with the corresponding $\hat{S}^2$ expectation values reported in Table V. As noted earlier, most of the CC methods employed in this work identify $^2\Pi$ as the ground state of C_4H (at its optimized geometry), but we have elected to compute vertical excitation energies relative to the optimized geometry of the lowest $^2\Sigma^+$ state (which is nearly degenerate) in part for easier comparison to the corresponding states of C_2H. The Hartree–Fock configuration of the $^2\Sigma^+$ state is (core) $8\sigma^2 1\pi^4 2\pi^4 9\sigma$. The key virtual MOs for the states given in the table are the singly occupied 9σ, the valence $3\pi^*$, and several low-lying Rydberg orbitals, including the $3s$, $3p\sigma$, and a pair of nearly degenerate $3p\pi$ orbitals (one centered on C_3 and the other on the C_2-C_3 bond). Some higher-lying states given in the table include minor contributions into the $10\sigma^*$ and the Rydberg $4s$.

Similar to the observations above for C_2H, all of the states obtained for C_4H exhibit some Rydberg character in the canonical Hartree–Fock MO basis. Even the lowest-lying excited state, $1\ ^2\Pi$, which is dominated by a $2\pi\rightarrow9\sigma$ transition (0.81 β), still includes a non-negligible contribution from a $2\pi\rightarrow3p\sigma$ transition. Although the modest AEL for the $1\ ^2\Pi$ state of 1.09 is similar to that in C_2H (1.08), the choice of reference determinant is even more significant for this transition in C_4H than for C_2H, with a U-R difference at the CCSD level of theory of more than 0.4 eV. This difference, which can be attributed to the large spin contamination in the reference state, decreases to 0.13 eV at the CC3 level, as expected, but is still larger than that in C_2H. The ROHF-

TABLE IV. Vertical excitation energies (eV), state assignments, characters, and AELs (from the ROHF-CCSD level) of C_4H relative to the lowest $^2\Sigma^+$ state at various levels of theory with the aug-cc-pVDZ basis set.

State assignment	Excitation character		Vertical excitation energy				AEL
			UHF-CCSD	UHF-CC3	ROHF-CCSD	ROHF-CC3	
$1\ ^2\Pi$	$2\pi\rightarrow9\sigma$	$(0.81\ \beta)$	0.904	0.483	0.487	0.358	1.09
	$1\pi\rightarrow9\sigma$	$(0.27\ \beta)$					
	$2\pi\rightarrow3p\sigma$	$(0.26\ \beta)$					
	$2\pi\rightarrow3\pi^*\ 2\pi\rightarrow9\sigma$	$(0.10\ \alpha\beta)$					
$2\ ^2\Pi$	$1\pi\rightarrow9\sigma$	$(0.75\ \beta)$	4.660	3.702	4.336	3.510	1.22
	$1\pi\rightarrow3p\sigma$	$(0.24\ \beta)$					
	$2\pi\rightarrow3\pi^*\ 2\pi\rightarrow9\sigma$	$(0.14\ \alpha\beta;\ 0.10\ \alpha\beta)$					
	$1\pi\rightarrow3\pi^*\ 1\pi\rightarrow9\sigma$	$(0.12\ \alpha\beta)$					
	$2\pi\rightarrow3p\pi\ 2\pi\rightarrow9\sigma$	$(0.12\ \alpha\beta)$					
	$2\pi\rightarrow3\pi^*\ 1\pi\rightarrow9\sigma$	$(0.10\ \alpha\beta)$					
$1\ ^4\Sigma^+$	$2\pi\rightarrow3\pi^*$	$(0.35\ \alpha;\ 0.30\ \beta;\ 0.19\ \alpha\beta)$	4.268	4.074	4.090	4.005	1.10
	$2\pi\rightarrow3p\pi$	$(0.25\ \beta;\ 0.11\ \alpha\beta)$					
$1\ ^4\Delta$	$2\pi\rightarrow3\pi^*$	$(0.38\ \alpha;\ 0.31\ \beta;\ 0.17\ \alpha\beta)$	5.097	4.901	4.996	4.859	1.10
	$2\pi\rightarrow3p\pi$	$(0.20\ \alpha;\ 0.25\ \beta)$					
$1\ ^4\Sigma^-$	$2\pi\rightarrow3\pi^*$	$(0.41\ \alpha;\ 0.30\ \beta;\ 0.16\ \alpha\beta)$	5.670	5.452	5.573	5.407	1.10
	$2\pi\rightarrow3p\pi$	$(0.21\ \alpha;\ 0.23\ \beta)$					
$2\ ^2\Sigma^+$	$2\pi\rightarrow3\pi^*$	$(0.40\ \alpha\beta)$	7.735	5.908	7.368	5.607	1.81
	$2\pi\rightarrow3p\pi$	$(0.21\ \alpha\beta)$					
	$9\sigma\rightarrow3\pi^*\ 2\pi\rightarrow3p\sigma$	$(0.15\ \alpha\beta)$					
$1\ ^2\Sigma^-$	$2\pi\rightarrow3\pi^*$	$(0.39\ \alpha;\ 0.37\ \beta)$	5.829	5.683	5.783	5.699	1.08
	$2\pi\rightarrow3p\pi$	$(0.27\ \beta)$					
$1\ ^2\Delta$	$2\pi\rightarrow3\pi^*$	$(0.42\ \alpha;\ 0.35\ \beta)$	6.064	5.941	6.028	5.953	1.08
	$2\pi\rightarrow3p\pi$	$(0.20\ \alpha;\ 0.24\ \beta)$					
$2\ ^4\Sigma^+$	$1\pi\rightarrow3\pi^*$	$(0.31\ \alpha;\ 0.27\ \beta;\ 0.17\ \alpha\beta)$	6.367	6.506	6.261	6.394	1.18
	$1\pi\rightarrow3p\pi$	$(0.20\ \beta)$					
	$2\pi\rightarrow3\pi^*$	$(0.13\ \alpha\beta)$					
$2\ ^4\Sigma^-$	$2\pi\rightarrow3\pi^*$	$(0.41\ \alpha\beta)$	7.876	7.450	7.807	7.182	1.14
	$1\pi\rightarrow3\pi^*$	$(0.26\ \alpha)$					
	$2\pi\rightarrow3p\pi$	$(0.19\ \alpha\beta)$					
	$9\sigma\rightarrow3\pi^*\ 2\pi\rightarrow3p\sigma$	$(0.16\ \alpha\beta)$					
$3\ ^2\Pi$	$2\pi\rightarrow3s$	$(0.72\ \beta)$	7.375	7.259	7.433	7.266	1.09
	$2\pi\rightarrow10\sigma^*$	$(0.35\ \beta)$					
	$2\pi\rightarrow4s$	$(0.31\ \beta)$					
	$2\pi\rightarrow3p\sigma$	$(0.28\ \beta)$					
$2\ ^4\Delta$	$1\pi\rightarrow3\pi^*$	$(0.33\ \alpha;\ 0.28\ \beta;\ 0.16\ \alpha\beta)$	7.289	6.864	7.201	7.280	1.15
	$1\pi\rightarrow3p\pi$	$(0.21\ \beta)$					
	$2\pi\rightarrow3\pi^*$	$(0.15\ \alpha\beta)$					
$4\ ^2\Pi$	$2\pi\rightarrow3s$	$(0.71\ \alpha;\ 0.14\ \beta;\ 0.21\ \alpha\beta)$	7.772	7.533	7.742	7.502	1.10
	$2\pi\rightarrow10\sigma^*$	$(0.36\ \alpha;\ 0.11\ \alpha\beta)$					
	$2\pi\rightarrow4s$	$(0.28\ \alpha)$					
	$2\pi\rightarrow3p\sigma$	$(0.20\ \alpha)$					

CC3 excitation energy of 0.36 eV, which we consider to be the most accurate among the CC methods considered here, is comparable to the value of 0.44 eV reported by Graf, Geiss, and Leutwyler[45] at the CASPT2/cc-pVQZ level of theory (at the MCSCF optimized geometry) using a (9,9) active space. Meanwhile, the TD-B3LYP level of theory yields an unphysical negative value for the square of the excitation energy.

The 2 $^2\Pi$ state is identified at 3.51 eV at the ROHF-CC3 level of theory, with a U-R difference of ca. 0.3 eV at the CCSD level (reduced to 0.19 eV at the CC3 level) and an AEL of 1.22. This state is similar in composition to the 1 $^2\Pi$ state in that it is dominated by a transition out of a valence π orbital into the singly occupied 9σ, and it also exhibits some

Rydberg character. Furthermore, Graf and co-workers[45] report a CASPT2/cc-pVQZ excitation energy for this state of 3.31 eV, in relatively good agreement with the CC results reported here. However, the good comparison between the CC and CASPT2 results does not continue further. Specifically, while Graf, Geiss, and Leutwyler[45] find five $^2\Pi$ states below 7.0 eV, we find only the two described above. The 3 $^2\Pi$ has an ROHF-CC3 excitation energy of 7.27 eV, while CASPT2/cc-pVQZ places it more than 2.5 eV lower at 4.71 eV.

As was observed for C_2H, the discrepancies between the CC and multireference (MR) results likely arise from the lack of spin adaptation of the former and the choice of active space in the latter. The most glaring impact of triples occurs

TABLE V. $\langle \hat{S}^2 \rangle$ values of excited states of C_4H at the EOM-CCSD/aug-cc-pVDZ level of theory. States marked in italics involve unbalanced contributions from low-spin determinants depicted schematically in Fig. 2.

State	UHF-EOM-CCSD	ROHF-EOM-CCSD
$1\,^2\Pi$	0.866	0.756
$2\,^2\Pi$	0.867	0.762
$1\,^4\Sigma^+$	3.191	3.253
$1\,^4\Delta$	3.072	3.203
$1\,^4\Sigma^-$	2.781	3.077
$2\,^2\Sigma^+$	*2.024*	*1.612*
$1\,^2\Sigma^-$	*1.104*	*0.857*
$1\,^2\Delta$	*0.879*	*0.763*
$2\,^4\Sigma^+$	3.030	2.852
$2\,^4\Sigma^-$	*2.313*	*2.431*
$3\,^2\Pi$	*2.059*	*2.077*
$2\,^4\Delta$	2.927	2.873
$4\,^2\Pi$	*1.835*	*1.708*

for the $2\,^2\Sigma^+$ state, with a shift between CCSD and CC3 of more than 1.8 eV with the UHF reference determinant. This state also exhibits the largest AEL (1.81) among the excited states below 8 eV, and its $\hat{S}^2$ expectation value lies intermediate between pure doublet and quartet values (and differs significantly between UHF and ROHF references at 2.024 and 1.612, respectively). The dominant excitation to this state in C_4H is the valence $2\pi \rightarrow 3\pi^*$ ($\alpha\beta$ double excitation) transition with little contribution from the $8\sigma \rightarrow 9\sigma$ transition, while in C_2H, the analogous $4\sigma \rightarrow 5\sigma$ transition is significant. Furthermore, while the large AEL in C_2H of 1.54 results in a (UHF) CCSD to CC3 difference of ca. 0.8 eV, the corresponding difference in C_4H increases to more than 1.8 eV. The U-R difference, on the other hand, is smaller (and comparable to that of the $1\,^2\Pi$ state) at 0.37 eV for CCSD and 0.30 eV for CC3. In the CASPT2 computations of Graf and co-workers,[45] the active space consisted of nine electrons in nine orbitals for lower-lying Σ and Π states, extended to eleven orbitals for Δ and higher-lying Σ states, and the CASPT2 configuration expansion was necessarily truncated due to resource limitations for the larger active

space. However, Graf *et al.* carried out a test of their active space choices for the $2\,^2\Sigma^+$ state, in particular, and found little sensitivity, lending greater confidence in the MR results for this state.

Table VI summarizes EOM-CCSD/aug-cc-pVTZ, /d-aug-cc-pVDZ, /t-aug-cc-pVDZ vertical excitation energies for the same 13 excited states (given in the same order as in Table IV). As observed for C_2H, the basis-set dependence of these states is small for the states dominated by valence-orbital transitions, and the largest shift between aug-cc-pVDZ and aug-cc-pVTZ occurs for the problematic $2\,^2\Sigma^+$ state, with the larger basis set producing an increase in the excitation energy of 0.34 eV at the UHF-CCSD level of theory. Additional diffuse functions stabilize those states dominated by Rydberg transitions, though the shifts in the excitation energies are smaller compared to C_2H. Thus, we note that the often-substantial disagreement between MR methods (in this case, the CASPT2 results of Graf and co-workers) and the CC3 data reported here are apparently not due to inadequacies in the basis set.

IV. CONCLUSIONS

We have examined the ability of high-level coupled-cluster methods (specifically the CCSD and CC3 approaches) for the computation of vertical excitation energies of the C_2H and C_4H $^2\Sigma^+$ radicals, both of which are relevant to interstellar chemistry. Two diagnostics—the difference between the UHF- and ROHF-based properties (the U-R difference) and the AEL—give us some insight into the quality of the resulting excitation energies. Computations of 16 excited states of C_2H and 13 states of C_4H demonstrate that the CCSD level of theory in the conventional UHF- and ROHF-based formalisms is not adequate for describing many excited states of radicals, unlike the case for closed-shell species, where the CCSD method typically yields rather high accuracy. Even for some low-lying valence-dominated states, the role of double excitations can be significant for even a qualitatively correct description of the transition, thus em-

TABLE VI. Vertical excitation energies (eV), state assignments, and AELs of C_4H relative to the ground $^2\Sigma^+$ state at the EOM-CCSD level of theory with the aug-cc-pVTZ, d-aug-cc-pVDZ, and t-aug-cc-pVDZ basis sets.

| State assignment	aug-cc-pVTZ			d-aug-cc-pVDZ		t-aug-cc-pVDZ	
	UHF	ROHF	AEL	UHF	ROHF	UHF	ROHF
$1\,^2\Pi$	0.913	0.464	1.09	0.889	0.468	0.889	0.468
$2\,^2\Pi$	4.709	4.363	1.21	4.649	4.322	4.649	4.322
$1\,^4\Sigma^+$	4.301	4.120	1.09	4.271	4.092	4.271	4.092
$1\,^4\Delta$	5.061	4.952	1.09	5.098	4.997	5.098	4.997
$1\,^4\Sigma^-$	5.622	5.525	1.09	5.669	5.571	5.669	5.571
$2\,^2\Sigma^+$	8.075	7.674	1.84	7.761	7.391	7.735	7.368
$1\,^2\Sigma^-$	5.751	5.686	1.08	5.828	5.781	5.828	5.781
$1\,^2\Delta$	5.991	5.944	1.08	6.061	6.024	6.061	6.024
$2\,^4\Sigma^+$	6.395	6.295	1.14	6.370	6.264	6.369	6.264
$2\,^4\Sigma^-$	7.811	7.747	1.12	7.874	7.805	7.873	7.805
$3\,^2\Pi$	7.464	7.519	1.09	7.294	7.347	7.293	7.346
$2\,^4\Delta$	7.240	7.153	1.12	7.289	7.202	7.289	7.202
$4\,^2\Pi$	7.846	7.819	1.09	7.680	7.655	7.679	7.654
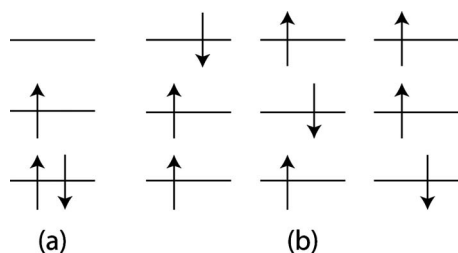
FIG. 2. Slater determinants contributing in zeroth order to (a) the doublet ground state and (b) $M_S = 1/2$ components of either a doublet or quartet excited state. Among the determinants depicted in (b), the first and third arise from single (spin-orbital) excitations relative to the reference determinant in (a), while the second is a "spin-flip" double excitation.

phasizing the need for correlation models that incorporate at least some estimate of connected triple excitations.

Spin contamination is substantial in many of the states, precluding definitive state assignments in some cases. The fundamental inadequacy of the spin-orbital coupled-cluster approach for such cases can be understood in terms of Fig. 2, which provides a schematic depiction of the determinants contributing to a zeroth-order description of both the ground/ reference state [denoted as (a) in the figure] and the $M_S = 1/2$ components of some of the quartet and doublet states of C_2H and C_4H [(b) in the figure]. Excited states whose leading contribution involving either an α-spin single-excitation from the singly occupied orbital or a β-spin single excitation into the singly occupied orbital tend to be relatively well described by the coupled-cluster methods used in this work. However, those states involving significant contributions from single excitations out of the doubly occupied orbitals into unoccupied orbitals produce low-spin determinants involving three unpaired electrons, such as those depicted in the first and third determinants in (b) in Fig. 2. Such determinants must be accompanied by the second determinant in (b) in order to obtain either the correct doublet or quartet state; however, in the spin-orbital formulation, this determinant is a double excitation relative to the reference determinant in (a) and thus is not treated in a balanced manner relative to the other two. In such cases, which we have identified by italics in Tables II and V, the corresponding coupled-cluster excitation energies may not be reliable. The CC3 method partly accounts for such excitations, but even higher levels of theory and/or expressly spin-adapted formalisms will be necessary in later studies in order to determine whether convergence has been reached in the correlated space. Future directions for this project include the application of the CC3 model to larger molecules, particularly those recently suggested as candidates for the carriers of the DIBs.[86]

ACKNOWLEDGMENTS

[1] H. Beckers, S. Esser, T. Metzroth, M. Behnke, H. Willner, J. Gauss, and J. Hahn, Chem.-Eur. J. **12**, 832 (2006).
[2] S. Green, J. A. Montgomery, and P. Thaddeus, Astrophys. J. **193**, L89 (1974).
[3] M. Guélin and P. Thaddeus, Astrophys. J. **212**, L81 (1977).
[4] S. Wilson and S. Green, Astrophys. J. **212**, L87 (1977).
[5] M. C. McCarthy, A. J. Apponi, V. D. Gordon, C. A. Gottlieb, P. Thaddeus, T. D. Crawford, and J. F. Stanton, J. Chem. Phys. **111**, 6750 (1999).
[6] S. Thorwirth, M. C. McCarthy, C. A. Gottlieb, P. Thaddeus, H. Gupta, and J. F. Stanton, J. Chem. Phys. **123**, 054326 (2005).
[7] S. Thorwirth, J. Gauss, M. McCarthy, F. Shindo, and P. Thaddeus, Chem. Commun. (Cambridge) **2008**, 5292.
[8] J. P. Maier, Chem. Soc. Rev. **26**, 21 (1997).
[9] J. P. Maier, J. Phys. Chem. **102**, 3462 (1998).
[10] M. C. McCarthy and P. Thaddeus, Chem. Soc. Rev. **30**, 177 (2001).
[11] H. Reisler and A. I. Krylov, Int. Rev. Phys. Chem. **28**, 267 (2009).
[12] H. Köppel, W. Domcke, and L. S. Cederbaum, Adv. Chem. Phys. **57**, 59 (1984).
[13] D. R. Yarkony, Acc. Chem. Res. **31**, 511 (1998).
[14] A. Hazra and M. Nooijen, Phys. Chem. Chem. Phys. **7**, 1759 (2005).
[15] T. Ichino, S. W. Wren, K. M. Vogelhuber, A. J. Gianola, W. C. Lineberger, and J. F. Stanton, J. Chem. Phys. **129**, 084310 (2008).
[16] F. Salama, G. A. Galazutdinov, J. Krelowski, L. J. Allamandola, and F. A. Musaev, Astrophys. J. **526**, 265 (1999).
[17] P. J. Sarre, J. Mol. Spectrosc. **238**, 1 (2006).
[18] L. M. Hobbs, D. G. York, T. P. Snow, T. Oka, J. A. Thorburn, M. Bishof, S. D. Friedman, B. J. McCall, B. Rachford, P. Sonnentrucker, and D. E. Welty, Astrophys. J. **680**, 1256 (2008).
[19] M. Kaźmierczak, P. Gnacinski, M. R. Schmidt, G. Galazutdinov, A. Bondar, and J. Krelowski, Astron. Astrophys. **498**, 785 (2009).
[20] X. F. Tan, Spectrochim. Acta, Part A **71**, 2005 (2009).
[21] R. J. Bartlett and M. Musial, Rev. Mod. Phys. **79**, 291 (2007).
[22] T. D. Crawford and H. F. Schaefer, in *Reviews in Computational Chemistry*, edited by K. B. Lipkowitz and D. B. Boyd (Wiley, New York, 2000), Vol. 14, pp. 33–136.
[23] T. J. Lee and G. E. Scuseria, in *Quantum Mechanical Electronic Structure Calculations with Chemical Accuracy*, edited by S. R. Langhoff (Kluwer, Dordrecht, 1995), pp. 47–108.
[24] T. Helgaker, T. A. Ruden, P. Jørgensen, J. Olsen, and W. Klopper, J. Phys. Org. Chem. **17**, 913 (2004).
[25] H. Koch, O. Christiansen, P. Jørgensen, A. M. S. de Merás, and T. Helgaker, J. Chem. Phys. **106**, 1808 (1997).
[26] O. Christiansen, H. Koch, and P. Jørgensen, J. Chem. Phys. **103**, 7429 (1995).
[27] K. Hald, P. Jørgensen, O. Christiansen, and H. Koch, J. Chem. Phys. **116**, 5963 (2002).
[28] C. E. Smith, R. A. King, and T. D. Crawford, J. Chem. Phys. **122**, 054110 (2005).
[29] K. D. Tucker, M. L. Kutner, and P. Thaddeus, Astrophys. J. **193**, L115 (1974).
[30] M. Guélin, S. Green, and P. Thaddeus, Astrophys. J. **224**, L27 (1978).
[31] A. E. Douglas, Nature (London) **269**, 130 (1977).
[32] J. Fulara, D. Lessen, P. Freivogel, and J. P. Maier, Nature (London) **366**, 439 (1993).
[33] J. K. G. Watson, Astrophys. J. **437**, 678 (1994).
[34] J. Fulara and J. Krelowski, New Astron. Rev. **44**, 581 (2000).
[35] T. W. Schmidt and R. G. Sharp, Aust. J. Chem. **58**, 69 (2005).
[36] H. Gupta, C. A. Gottlieb, M. C. McCarthy, and P. Thaddeus, Astrophys. J. **691**, 1494 (2009).
[37] A. Heikkilä, L. E. B. Johansson, and H. Olofsson, Astron. Astrophys. **344**, 817 (1999).
[38] T. S. Zwier and M. Allen, Icarus **123**, 578 (1996).

[39] It should be noted that many of the states examined in this work, such as those with higher spin multiplicities and strong double-excitation character, while interesting from the perspective of benchmarking theoretical methods, are not of practical importance for interstellar investigation.

[40] S.-K. Shih and S. D. Peyerimhoff, J. Mol. Spectrosc. **64**, 167 (1977).

[41] S.-K. Shih, S. D. Peyerimhoff, and R. J. Buenker, J. Mol. Spectrosc. **74**, 124 (1979).

[42] A. G. Koures and L. B. Harding, J. Phys. Chem. **95**, 1035 (1991).

[43] D. E. Woon, Chem. Phys. Lett. **244**, 45 (1995).

[44] A. L. Sobolewski and L. Adamowicz, J. Chem. Phys. **102**, 394 (1995).

[45] S. Graf, J. Geiss, and S. Leutwyler, J. Chem. Phys. **114**, 4542 (2001).

[46] K. Raghavachari, G. W. Trucks, J. A. Pople, and M. Head-Gordon, Chem. Phys. Lett. **157**, 479 (1989).

[47] J. Gauss, J. F. Stanton, and R. J. Bartlett, J. Chem. Phys. **95**, 2623 (1991).

[48] J. D. Watts, J. Gauss, and R. J. Bartlett, Chem. Phys. Lett. **200**, 1 (1992).

[49] J. S. Binkley, J. A. Pople, and P. S. Dobosh, Mol. Phys. **28**, 1423 (1974).

[50] J. Gauss, W. J. Lauderdale, J. F. Stanton, J. D. Watts, and R. J. Bartlett, Chem. Phys. Lett. **182**, 207 (1991).

[51] W. J. Lauderdale, J. F. Stanton, J. Gauss, J. D. Watts, and R. J. Bartlett, Chem. Phys. Lett. **187**, 21 (1991).

[52] J. D. Watts, J. Gauss, and R. J. Bartlett, J. Chem. Phys. **98**, 8718 (1993).

[53] M. Rittby and R. J. Bartlett, J. Phys. Chem. **92**, 3033 (1988).

[54] J. F. Stanton and J. Gauss, J. Chem. Phys. **101**, 8938 (1994).

[55] T. H. Dunning, J. Chem. Phys. **90**, 1007 (1989).

[56] J. F. Stanton and R. J. Bartlett, J. Chem. Phys. **98**, 7029 (1993).

[57] A. I. Krylov, Annu. Rev. Phys. Chem. **59**, 433 (2008).

[58] H. J. Monkhorst, Int. J. Quantum Chem., Symp. **11**, 421 (1977).

[59] D. Mukherjee and P. K. Mukherjee, Chem. Phys. **39**, 325 (1979).

[60] J. B. Foresman, M. Head-Gordon, J. A. Pople, and M. J. Frisch, J. Phys. Chem. **96**, 135 (1992).

[61] M. E. Casida, C. Jamorski, K. C. Casida, and D. R. Salahub, J. Chem. Phys. **108**, 4439 (1998).

[62] A. D. Becke, J. Chem. Phys. **98**, 5648 (1993).

[63] C. Lee, W. T. Yang, and R. G. Parr, Phys. Rev. B **37**, 785 (1988).

[64] P. J. Stephens, F. J. Devlin, C. F. Chabalowski, and M. J. Frisch, J. Phys. Chem. **98**, 11623 (1994).

[65] T. D. Crawford, C. D. Sherrill, E. F. Valeev, J. T. Fermann, R. A. King, M. L. Leininger, S. T. Brown, C. L. Janssen, J. P. Kenny, E. T. Seidl, and W. D. Allen, J. Comput. Chem. **28**, 1610 (2007).

[66] CFOUR, a quantum chemical program package written by J. F. Stanton, J. Gauss, M. E. Harding, P. G. Szalay, with contributions from A. A. Auer, R. J. Bartlett, U. Benedikt, C. Berger, D. E. Bernholdt, Y. J. Bomble, O. Christiansen, M. Heckert, O. Heun, C. Huber, T.-C. Jagau, D. Jonsson, J. Juslius, K. Klein, W. J. Lauderdale, D. A. Matthews, T. Metzroth, D. P. O'Neill, D. R. Price, E. Prochnow, K. Ruud, F. Schiffmann, S. Stopkowicz, A. Tajti, J. Vázquez, F. Wang, J. D. Watts, and the integral packages MOLECULE (J. Almlöf and P. R. Taylor), PROPS (P. R. Taylor), ABACUS (T. Helgaker, H. J. Aa. Jensen, P. Jørgensen, and J. Olsen), and ECP routines by A. V. Mitin and C. van Wüllen. For the current version, see http://www.cfour.de.

[67] M. J. Frisch, G. W. Trucks, H. B. Schlegel *et al.*, GAUSSIAN03, Gaussian, Inc., Pittsburg, PA, 2003.

[68] R. A. Kendall, T. H. Dunning, and R. J. Harrison, J. Chem. Phys. **96**, 6796 (1992).

[69] W. R. M. Graham, K. I. Dismuke, and W. Weltner, J. Chem. Phys. **60**, 3817 (1974).

[70] K. W. Chang and W. R. M. Graham, J. Chem. Phys. **76**, 5238 (1982).

[71] M. Kolbuszewski, Astrophys. J. **432**, L63 (1994).

[72] J. Natterer and W. Koch, Mol. Phys. **84**, 691 (1995).

[73] Q. Cui and K. Morokuma, J. Chem. Phys. **108**, 626 (1998).

[74] M. C. van Hemert and E. F. van Dishoeck, Chem. Phys. **343**, 292 (2008).

[75] J. F. Stanton, J. Chem. Phys. **101**, 371 (1994).

[76] A. I. Krylov, J. Chem. Phys. **113**, 6052 (2000).

[77] F. Pauzat, Y. Ellinger, and A. D. McLean, Astrophys. J. **369**, L13 (1991).

[78] J. H. Kiefer, S. S. Sidhu, R. D. Kern, K. Xie, H. Chen, and L. B. Harding, Combust. Sci. Technol. **82**, 101 (1992).

[79] K. I. Dismuke, W. R. M. Graham, and W. Weltner, J. Mol. Spectrosc. **57**, 127 (1975).

[80] S. Yamamoto, S. Saito, M. Guèlin, J. Cernicharo, H. Suzuki, and M. Ohishi, Astrophys. J. **323**, L149 (1987).

[81] L. N. Shen, T. J. Doyle, and W. R. M. Graham, J. Chem. Phys. **93**, 1597 (1990).

[82] M. C. McCarthy, C. A. Gottlieb, P. Thaddeus, M. Horn, and P. Botschwina, J. Chem. Phys. **103**, 7820 (1995).

[83] K. Hoshina, H. Kohguchi, Y. Ohshima, and Y. Endo, J. Chem. Phys. **108**, 3465 (1998).

[84] T. R. Taylor, C. Xu, and D. M. Neumark, J. Chem. Phys. **108**, 10018 (1998).

[85] P. Szalay and J. Gauss, J. Chem. Phys. **112**, 4027 (2000).

[86] C. D. Ball, M. C. McCarthy, and P. Thaddeus, Astrophys. J. **529**, L61 (2000).